SUPPLEMENT MATERIAL

MATERIALS AND METHODS

Neonatal Rat Ventricular Monolayers

Neonatal Rat Ventricular Myocytes (NRVM) were obtained as described in.[1] One-two day old Sprague-Dawley Rats (Charles River, MA) were euthanized and their hearts removed from the thoracic cavity. The hearts were finely minced, and enzymatically digested.[1] The enzymatic fractions were combined to 20mL of supplemented M199 containing 10%FBS. Fractions were spun down and pellets resuspended in supplemented M199 containing 10%FBS, and filtered through a 40µm filter. Cells were subjected to a 2h pre-plating at 37°C 5%CO_2 and the cell suspension was then passed through a 70µm filter. Cells were then counted and platted in 35mm dishes, 18mm coverslips, or 14mm glass-bottom dishes pre-coated with Collagen type IV. BrDU was added to prevent fibroblast proliferation. Media change was performed every 24h for the first 48h and every 48h thereafter.

Co-Immunoprecipitation

Co-IP experiments were performed as previously described.[1] Briefly, heart lysates were homogenized in lysis buffer and centrifuged at 3500 rpm for 15min. The supernatant was retained and exposed to Protein A/G beads for 30min at 4°C, followed by centrifugation at 3500rpm for 5min. The pre-cleared supernatant was exposed to beads coated with the antibodies of interest for one hour at 4°C, followed by centrifugation (2500 rpm for 5 min) and re-suspension in lysis buffer. The last step was repeated three times to clear the solvent of unbound material. The final pellet was resuspended in 6x Laemmli buffer and separated by conventional SDS PAGE electrophoresis and transferred for protein detection by immunoblot (see also below). Antibodies used as precipitants were Mouse PKP2 (Meridian Life Science), Rabbit Cx43 (Chemicon), Rabbit Ank-G (Santa Cruz Biotechnologies), PAN-Cadherin (Sigma). Antibodies for protein detection in these experiments were Mouse PKP2 (Meridian), Mouse Cx43-NT1 (Fred Hutchinson Cancer Researach Center), Mouse Ank-G (Neuromab), N-cadherin (BD Transduction).

Western Blot

Western blot analysis of protein content in cardiac cells was performed as previously described.[1] Briefly, 35mm NRVM monolayers were harvested in Tris-EGTA containing 5-10X protease inhibitors (Roche). Cells were spun for 3min at 4°C and pellets exposed to the lysis buffer for 30min at 4°C. After spinning for 3min at 4°C, the lysate was combined with 5X Sample Buffer. For PKP2 or Cx43 detection, samples were heated for 5min at 55°C (for Cx43) or 100°C (for PKP2), loaded in a 4-20% 15-well Tris-Glycine gel, and run at 120V. Proteins were transferred to a 0.45µm nitrocellulose membrane (120V; 90min). Membranes were blocked (5%NFM in T-PBS) for 1h at room temperature, and primary antibody incubated overnight at 4°C. Secondary antibodies were used for 45min at room temperature. For Nav1.5 or AnkG detection, samples were heated for 5min at 37°C, loaded in a 4-12% 15-well Tris-glycine gel, and run at 100V. Proteins were transferred to a 0.45µm nitrocellulose membrane at 4°C, 60mA, for 16h. Membranes were then blocked (5%NFM in T-TBS for Nav1.5 or 4%BSA in 0.2%Triton-Phosphate buffer, for AnkG) for 1h at room temperature. Primary antibodies were incubated overnight at 4°C in their respective blocking buffers. Secondary antibodies were used for 45min at room temperature. After the primary detection, membranes were stripped with Restore® (Thermo Scientific, 21059). Membranes were washed with T-PBS and blocked for 1h (5%NFM

T-PBS) at room temperature. Tubulin antibody was used as loading control. Primary antibodies used were: Rabbit Nav 1.5 (Alomone #ASC-005), Rabbit Ankyrin-G (kind gift from Dr. Vann Bennett- Duke University), Mouse PKP2 (Biodesign), Mouse Plakoglobin (Sigma), Mouse N-cadherin (BD Transduction), Mouse Cx43-NT1 (Fred Hutchinson Cancer Research Center), Mouse Tubulin (Hybridoma Bank at University of Iowa).

Protein Knockdown

Silencing oligos specific for rat PKP2 or AnkG were obtained from Dharmacon (Chicago, USA). Cardiac myocytes were transfected 24h post-plating with ON-TARGETplus SMARTpool siRNA specific for rat PKP2 (CCAAAUCUAGUAACGAAUA, CCACAUCGGUAGCUCGCAU, GAGGAAUUUGUCACGGAAU, AGUUUAAGAAGACGGACUU) or rat AnkG (AAGCAGAAGUGGUGCGGUA,GUGCGAAGAUCGACGCCAA,CCUUGUGAGCGGACGGAUA , UGGCAAUAGUAGCCGAUCA). Control for transfection was provided by using ON-TARGETplus Non-targeting siRNA. All transfections were performed according to the manufacturer's protocol using Dharmafect-1. Complete silencing of PKP2 and AnkG was observed at day 5 and day 6 post-transfection, respectively.

Immunofluorescence

Cells plated in 18mm glass coverslips or 14mm glass-bottom dishes were fixed in either 3% paraformaldehyde or cold ethanol for 5min depending on the protein of interest. For staining involving Nav1.5, blocking was done using 0.1% Triton in PBS containing 20% goat serum for 2h at room temperature. Primary antibodies were diluted in 0.1% Triton in PBS containing 5% goat serum and incubated overnight at 4°C. Primary antibodies were then washed with PBS and secondary antibodies were incubated for 1h at room temperature. For staining involving Ankyrin-G, blocking was done using 0.025% Triton in PBS containing 30% sucrose, 3% fish gelatin, and 20% goat serum for 2h at room temperature. Primary antibodies were diluted in 0.025% triton in PBS containing 30%sucrose, 3%fish gelatin, and 5% goat serum and incubated overnight at 4°C. Primaries were then washed with PBS and secondary antibodies were incubated for 1h at room temperature. Primary antibodies used were: Rabbit Nav1.5 (Alomone #ASC-005), Rabbit Ankyrin-G (Santa Cruz Biotechnologies), Mouse PKP2 (Biodesign), Mouse Plakoglobin (Sigma), Mouse N-cadherin (BD Transduction), Mouse Cx43-IF1 (Fred Hutchinson Cancer Research Center), Alexa Fluor 488 Phalloidin (Invitrogen). Secondary antibodies used were: Mouse Alexa Fluor 594, Rabbit Alexa Fluor 488, and DAPI (Molecular Probes). Image acquisition was done using Axioplan 2 bright field microscope (Zeiss) equipped with 63X Plan Apo Lenses or with Zeiss Inverted microscope equipped with 100X objective. All gains for the acquisition of comparable images were maintained constant.

Dispase Assay

The protocol to assess intercellular adhesion strength was modified from[2-5]. NRVMs were plated to confluency in 35mm dishes. Cells were washed with warm PBS, and then incubated with 1.2-2.4 U/mL Dispase at 37°C/5%CO_2 for 4h. Blebistatin (10μM) was added to the media to decrease cellular contraction. Fragmentation of the monolayer was induced by using an orbital shaker at 70rpm. Imaging of the monolayers was done using a Canon EOS Rebel Xsi Digital Camera containing a Sigma DC 17-70mm 1:2.8-4 MACRO HSM lens. In addition, a HDYA 72mm PL-CIR polarizing lens was used to minimize reflection. The camera was mounted on an inverted tripod and a remote switch was used to take the images to minimize external vibrations. Images were imported to a computer and Photoshop was used to enhance visualization by changing the mode to grayscale and turning the background black.

Patch Clamp Recordings

Measurement of junctional conductance between NRVM cell pairs followed conventional protocols.[1,6] Cells were recorded in the dual voltage clamp configuration. Each cell of the pair was independently voltage clamped to the same holding potential (-40mV). Cell 1 was stepped to +20mV, creating a potential difference of +60mV, during repetitive 10 s steps. The current applied by the voltage clamp circuit in cell 2 during the pulse in cell 1 was considered equal and opposite to the junctional current. Junctional conductance was calculated as per Ohm's Law. Protocols for sodium current recordings as in[1].

Optical Mapping

Optical Mapping experiments were performed as previously described.[1] Monolayers were stained with Di-8ANEEPS (40μM) for 15min at 37°C, washed one time with HBSS containing Ca and Mg, placed on a glass holder and kept at a constant temperature of 37°C. HBSS containing Ca and Mg at 37°C was superfused throughout the preparation during the recordings. A dichroic mirror was placed in-between the light source and the preparation, and signal was captured by an 80x80 pixel CCD camera placed under the preparation. An electrode was placed in the center of the dish and pacing stimulus was delivered at 1Hz increments until failure of 1:1 capture. Sampling rate for optical recording was 200-500 frames per second (2-5ms frame intervals) and a complete sample episode lasted 5 seconds (i.e., each movie was 5 seconds in duration). Conduction velocity was calculated from data on the entire 5-second episode. Pacing was done at 5 ms stimulation with 5 mV pulse. Off-line filtration was done using SCROLL software. Details on filtration parameters can be found elsewhere[7, 8].

Statistical Analysis

One-way ANOVA analysis followed by Bonferroni or Tukey tests were performed by using SPSS17 (Statistical Package for the Social Sciences, version 17; also known as PASW, Predictive Analytics Software). Statistical consultation was done by the University of Michigan-CSCAR (Center for Statistical Consultation and Research).

RESULTS

AnkG precipitates PKP2 in the absence of detectable N-cadherin

Co-immunoprecipitation of AnkG with PKP2 is shown in the main manuscript. Here, we sought to determine whether N-cadherin would also be consistently observed in an AnkG precipitate. Beads coated with antibodies against Cx43, AnkG or (in some cases) cadherin were presented to a heart lysate. Each precipitate was then probed with antibodies against PKP2, AnkG or N-cadherin. As shown in Online Figure I, we confirmed the presence of immunodetectable PKP2 in the AnkG precipitate (panels A and B; similar result as in Figure 1 of main manuscript). Yet, N-cadherin was not consistently observed (compare N-cadherin immunoblot in A, where no N-cadherin was found, versus B, where an N-cadherin signal was found in precipitates from AnkG as well as Cx43). These results complement those reported in Figures 1 and 3 of the manuscript. A discussion on the limitations of immunoprecipitation experiments is also presented in the manuscript.

Analysis of AnkG abundance in NRVMs in control conditions, or treated with AnkG-siRNA

Studies presented in this manuscript sought to determine the relevance of AnkG expression on the abundance, localization and function of proteins relevant to intercellular communication and/or sodium channel function. Online Figure II-A shows the compiled results obtained from the Western blot analysis of samples that were either untreated (UNT), or treated with oligonucleotides designed to prevent (AnkG-siRNA) or not prevent (ΦsiRNA) AnkG protein

expression. All values were measured relative to the band density obtained from untreated cells, corrected by a tubulin loading control (see raw data in main manuscript; e.g., Figure 2A and others). Collectively, the density of the bands detected by AnkG antibodies on samples from siRNA-treated cells was <5% of the band density in parallel samples that were untreated, or treated with a non-silencing construct. Moreover, for immunofluorescence experiments assessing the effect of AnkG silencing, cells were co-stained for AnkG and for the protein of interest. As shown in Online Figure II-B-C, AnkG co-localized with PKP2 at sites of cell contact in untreated cells. On the other hand, as shown by data in Online Figure III and also in the main manuscript, negligible AnkG-immuoreactive signal was detected from cells treated with the siRNA construct.

Intercellular adhesion strength after loss of PKP2 expression

Loss of AnkG expression led to a decrease in intercellular adhesion strength. Data on that regard are presented in the main manuscript (Figure 6). Examples of fragmentation of NRVM monolayers previously treated with PKP2-siRNA are also shown in the main text. Online Figure IV shows Western blots (panels A and B) confirming the efficiency of the siRNA construct (tubulin used as loading control). Panel C shows the collective data obtained from quantifying the number of fragments observed in the three experimental conditions, at time zero, 1 and three minutes of gentle agitation. Each symbol represents an individual experiment. Notice that the ordinate axis is interrupted to indicate that loss of PKP2 expression caused the disruption of the monolayer into more than 30 fragments, at which point individual fragments were difficult to resolve at the level of resolution of our recording system. Finally, Online Figure V confirms loss of AnkG expression in AnkG-siRNA-treated cells prepared in parallel with those used for the intercellular adhesion experiments presented in the main manuscript.

Sodium current after loss of AnkG expression in NRVMs.

Previous studies have documented that AnkG expression is relevant to sodium current properties[9,10] Confirmation of these observations in our experimental system (and within the time frame of our studies) is presented here. Panel A of Online Figure VI displays original current traces obtained from NRVMs treated either with siRNA for AnkG, or with a construct that did not affect AnkG expression (ΦsiRNA). Panels B, C and D reveal that loss of AnkG expression caused a reduction in sodium current amplitude (B) without changes in steady-state inactivation (C), or recovery from inactivation (D). Panel E presents data on the rate of current decay (measured by fitting an exponential function to the current traces obtained at a voltage command of -40 mV), and Panel F displays Western blot data confirming loss of AnkG expression in AnkG-siRNA-treated cells prepared in parallel with those used for the voltage clamp experiments. Altogether, we observed changes in sodium current properties and $Na_v1.5$ localization (main manuscript, Figure 7B) consistent with those previously reported. Overall, AnkG silencing caused changes on sodium current amplitude, gap junction communication (Figure 7A of manuscript) and intercellular adhesion strength.

AnkG knockdown and phalloidin staining

Our experiments revealed that AnkG had no effect on the abundance or distribution of N-cadherin, and of plakoglobin (Figure 3 of the main manuscript). Further evidence that the observed effects of AnkG knockdown were not reflecting a generalized loss of cell integrity is presented in Online Figure VII. In this case, NRVMs were stained with an antibody against phalloidin. The figure shows that cells treated with AnkG-siRNA showed a preserved cytoskeletal architecture similar to that of cells treated with the control construct (compare panels A and B of Online Figure VII).

AnkG and action potential propagation in monolayers of NRVMs.
Previous studies[9,10] and those presented here, support the notion that AnkG interacts with molecular complexes involved in electrical homeostasis. Yet, the role of AnkG on action potential propagation in cardiac cells remains undefined. Monolayers of NRVMs were paced at various frequencies with an electrode located in the center of the preparation. Conventional optical mapping methods were used to record electrical activity.[1] Results obtained from monolayers exposed to ΦsiRNA were used as control (n=8) and compared to those obtained from cells treated with the AnkG-siRNA construct (n=6). Loss of AnkG expression in the mapped monolayers was confirmed by Western blot following the conclusion of the electrophysiological experiment (Online Figure VIII). Isochrone maps are depicted in Online Figure IX-A. A plot of conduction velocity as a function of pacing frequency is presented in Online Figure IX-B. Small numbers above each data point indicate the number of preparations in which we were able to sustain a 1:1 stimulus:response ratio at that particular pacing frequency. The data show that loss of AnkG expression did not affect the velocity of action potential propagation in the range of pacing frequencies between 1 and 6 Hz. Yet, an increase in the pacing rate led to loss of 1:1 capture. In fact, we failed to command electrical activity in all AnkG-knockdown preparations at stimulation frequencies of 8Hz or higher (asterisks), whereas a 1:1 ratio was maintained for 4 out of the 8 control preparations paced at the same frequency. These results indicate that AnkG contributes to preservation of action potential propagation at high pacing frequencies.

DISCUSSION

Overall, our results suggest a functional and molecular interaction of AnkG with components of the desmosome, gap junctions and the VGSC complex. These interactions may be direct, or indirect (via additional intermediate molecules). Online Figure X is a diagram not intended as an exact representation of the molecular components but rather, a conceptualization of the fact that desmosomes, sodium channels and gap junctions may represent a functional unit at the intercalated disc.

The observation that AnkG silencing did not affect conduction velocity in NRVM monolayers seems surprising, given the known importance of AnkG on sodium current function and our observations confirming that loss of AnkG expression causes a redistribution of $Na_v1.5$ and a decrease in sodium current amplitude (Online Figure VI; see also[9,10]), as well as a decrease in junctional conductance. The mechanism(s) underlying these unexpected/interesting experimental observations are presently unknown and warrant further investigation. The mechanistic basis of a ‘propagation reserve’ in intact hearts is also still largely unknown.[11,12] It is possible that future use of this and other experimental models could serve at some point to elucidate respective mechanisms. Further characterization of the role of AnkG on cardiac propagation awaits availability of an animal model of AnkG deficiency, where electrophysiological parameters can be measured in an intact adult heart. Of note, although the studies of Lowe et al have indicated that AnkG is not relevant for preservation of calcium currents,[10] a possible role of AnkG on the function of other ionic currents in the heart cannot be discarded.

References

1. **Sato PY, Musa H, Coombs W, Guerrero-Serna G, Patino GA, Taffet SM, Isom LL, Delmar M. Loss of plakophilin-2 expression leads to decreased sodium current and slower conduction velocity in cultured cardiac myocytes. *Circ Res*. 2009;105:523-526**
2. **Huen AC, Park JK, Godsel LM, Chen X, Bannon LJ, Amargo EV, Hudson TY, Mongiu AK, Leigh IM, Kelsell DP, Gumbiner BM, Green KJ. Intermediate filament-membrane attachments function synergistically with actin-dependent contacts to regulate intercellular adhesive strength. *J Cell Biol*. 2002;159:1005-1017**
3. **Hudson TY, Fontao L, Godsel LM, Choi HJ, Huen AC, Borradori L, Weis WI, Green KJ. In vitro methods for investigating desmoplakin-intermediate filament interactions and their role in adhesive strength. *Methods Cell Biol*. 2004;78:757-786**
4. **Simpson CL, Kojima SI, Cooper-Whitehair V, Getsios S, Green KJ. Plakoglobin Rescues Adhesive Defects Induced by Ectodomain Truncation of the Desmosomal Cadherin Desmoglein 1. Implications for Exfoliative Toxin-Mediated Skin Blistering. *Am J Pathol*. 2010;November 12:*Ahead of print***
5. **Calautti E, Cabodi S, Stein PL, Hatzfeld M, Kedersha N, Dotto GP. Tyrosine Phosphorylation and Src Family Kinase Control Keratinocyte Cell-Cell Adhesion. *Journal of Cell Biology*. 1998;141:1449-1465**
6. **Verma V, Larsen BD, Coombs W, Lin X, Spagnol G, Sorgen PL, Taffet SM, Delmar M. Novel pharmacophores of connexin43 based on the "RXP" series of Cx43-binding peptides. *Circ Res*. 2009;105:176-184**
7. **Mironov SF, Vetter FJ, Pertsov AM. Fluorescence imaging of cardiac propagation: spectral properties and filtering of optical action potentials. *Am J Physiol Heart Circ Physiol*. 2006;291:H327-335**
8. **Gray RA, Jalife J, Panfilov A, Baxter WT, Cabo C, Davidenko JM, Pertsov AM. Nonstationary vortexlike reentrant activity as a mechanism of polymorphic ventricular tachycardia in the isolated rabbit heart. *Circulation*. 1995;91:2454-2469**
9. **Mohler PJ, Rivolta I, Napolitano C, LeMaillet G, Lambert S, Priori SG, Bennett V. Nav1.5 E1053K mutation causing Brugada syndrome blocks binding to ankyrin-G and expression of Nav1.5 on the surface of cardiomyocytes. *Proc Natl Acad Sci U S A*. 2004;101:17533-17538**
10. **Lowe JS, Palygin O, Bhasin N, Hund TJ, Boyden PA, Shibata E, Anderson ME, Mohler PJ. Voltage-gated Nav channel targeting in the heart requires an ankyrin-G dependent cellular pathway. *J Cell Biol*. 2008;180:173-186**
11. **van Veen TA, Stein M, Royer A, Le Quang K, Charpentier F, Colledge WH, Huang CL, Wilders R, Grace AA, Escande D, de Bakker JM, van Rijen HV. Impaired impulse propagation in Scn5a-knockout mice: combined contribution of excitability, connexin expression, and tissue architecture in relation to aging. *Circulation*. 2005;112:1927-1935**
12. **Stein M, van Veen TA, Remme CA, Boulaksil M, Noorman M, van Stuijvenberg L, van der Nagel R, Bezzina CR, Hauer RN, de Bakker JM, van Rijen HV. Combined reduction of intercellular coupling and membrane excitability differentially affects transverse and longitudinal cardiac conduction. *Cardiovasc Res*. 2009;83:52-60**

Online Figure I

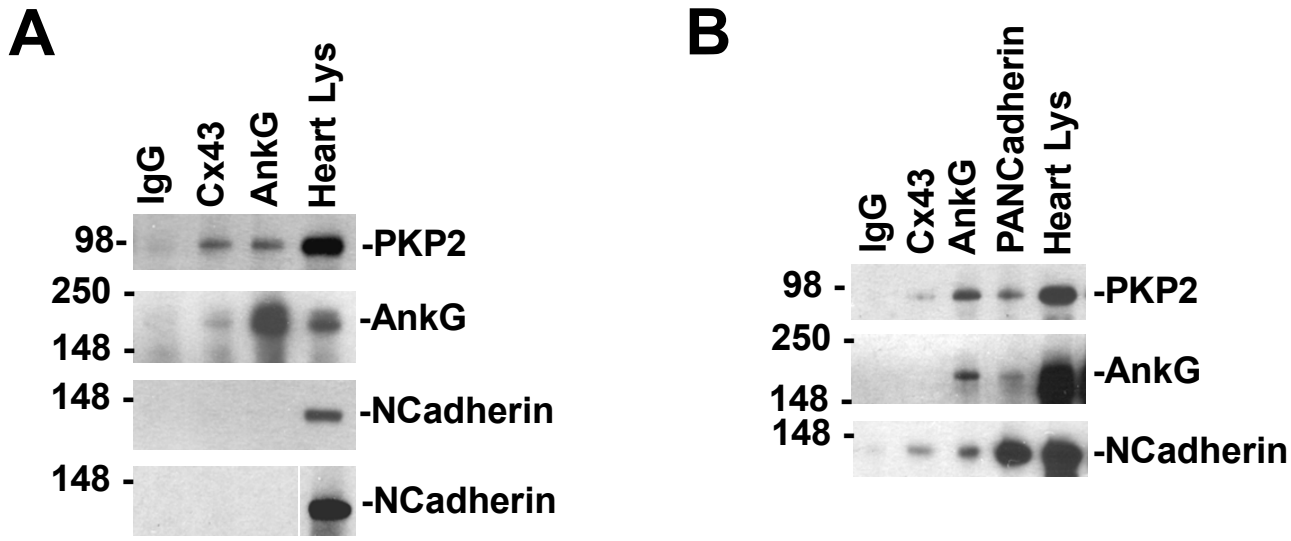

Online Figure I: A: Immunoblots of PKP2, AnkG, and N-cadherin (top to bottom) from samples exposed to protein A/G beads coated with rabbit IgG (negative control), Cx43, or AnkG antibodies. Heart lysate (right-most lane) was used as positive control. Blot shown at the bottom is overexposed to further demonstrate the absence of an N-cadherin immunoreactive signal in the precipitates. **B:** Similar experiment as in A. Immunoblots of PKP2, AnkG, and N-cadherin (from top to bottom) from samples exposed to protein A/G beads coated with rabbit IgG (negative control), Cx43, AnkG, or cadherin antibodies. Heart lysate (right lane) was used as positive control.

Online Figure II

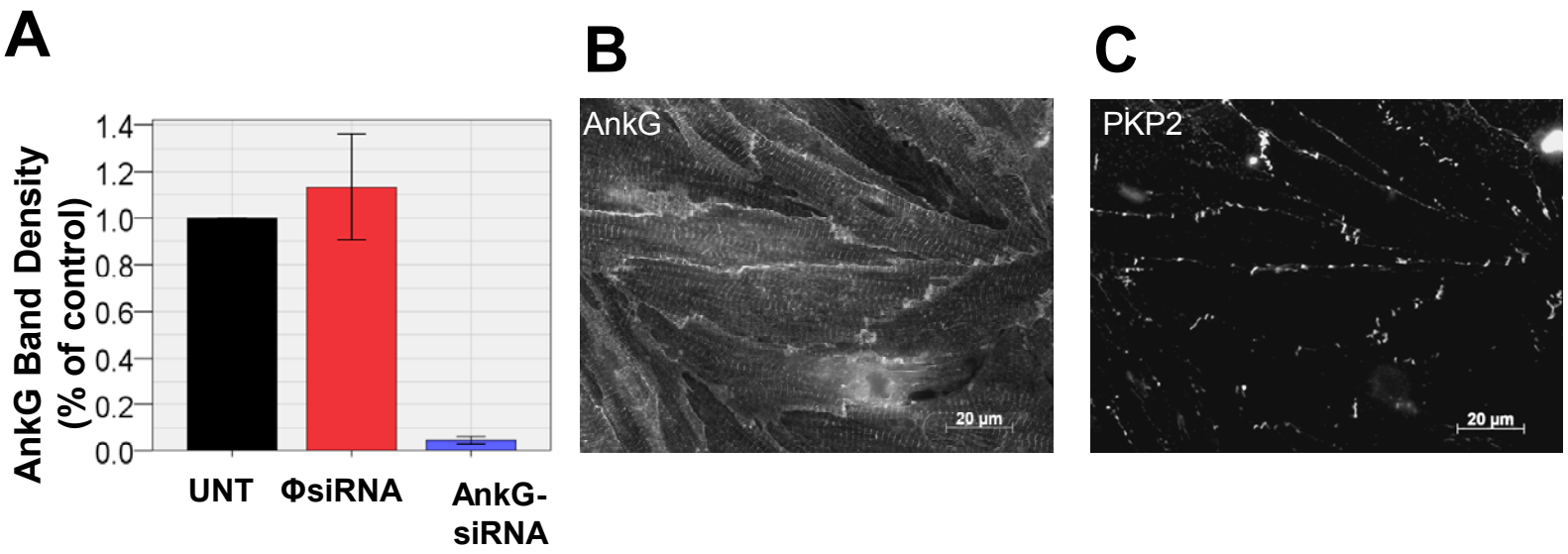

Online Figure II. A: Quantification of band densities in immunoblots treated with AnkG antibodies. Bars indicate the density of AnkG-immunoreactive bands in NRVMs. UNT: Untreated. ΦsiRNA, cells treated with an oligonucleotide that does not silence AnkG expression. AnkG-siRNA: cells treated with a construct designed to knockdown AnkG expression. All bands calibrated by density of a loading control (tubulin). Quantification was made relative to density of band in UNT lane, for each blot. Bars represent SEM**. B-C**: Co-localization of AnkG (B) and PKP2 (C) at sites of cell contact in untreated NRVMs.

Online Figure III

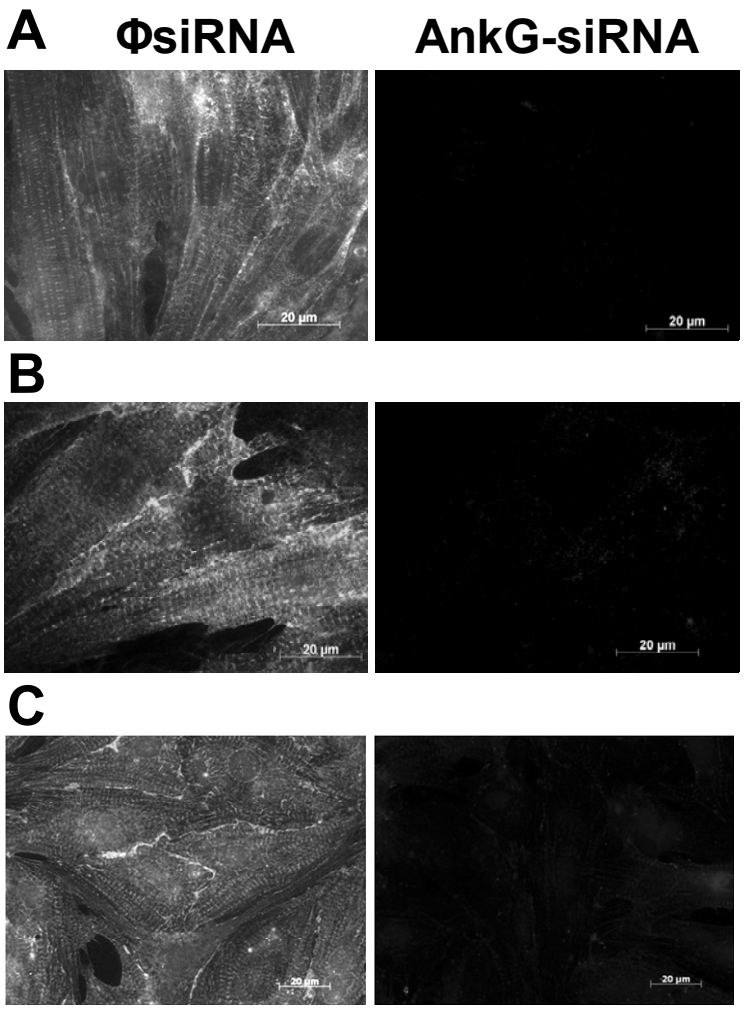

Online Figure III. Localization of AnkG-immunoreactive proteins in NRVM monolayers that were treated with a control oligonucleotide (ΦsiRNA) or with AnkG-siRNA. Panels **A, B and C** depict the same images as those used to illustrate the localization of plakoglobin, N-cadherin and Cx43 (respectively), and presented in the main manuscript (see Figures 3 and 7).

Online Figure IV

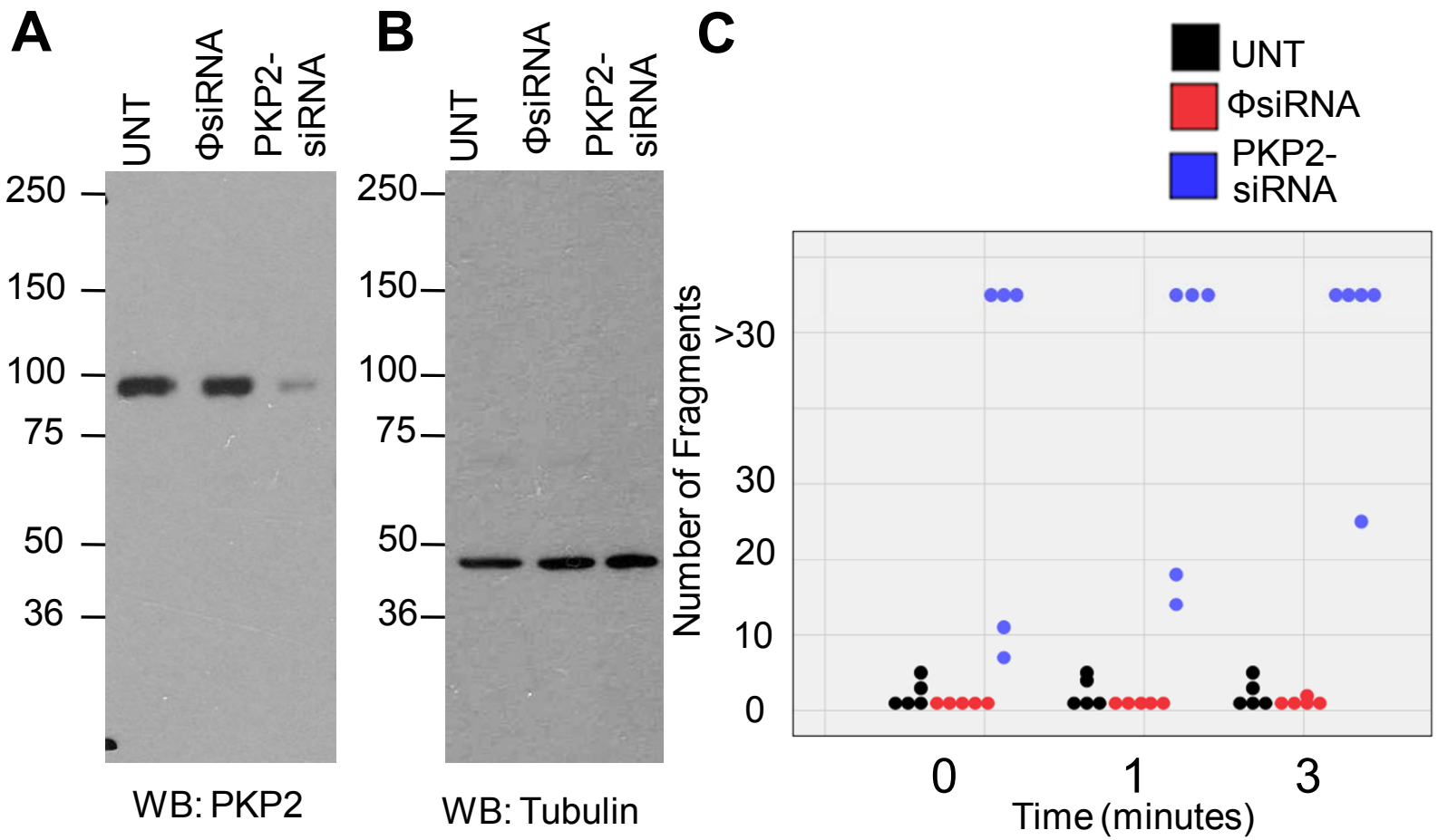

Online Figure IV: Panels **A** and **B**: Representative western blots of NRVM monolayers subjected to dispase to assess intercellular adhesion strength. Samples were untreated (UNT) or treated with ΦsiRNA or PKP2-siRNA. The membranes were probed for PKP2 (A) and tubulin (B) as a loading control. **C**: Numbers of fragments in monolayers previously left untreated (black symbols) or treated with the constructs specified in the inset (red for ΦsiRNA and blue for PKP2-siRNA). Samples that fragmented in more than 30 units are only reported as ">30." Each data point corresponds to an individual experiment.

Online Figure V

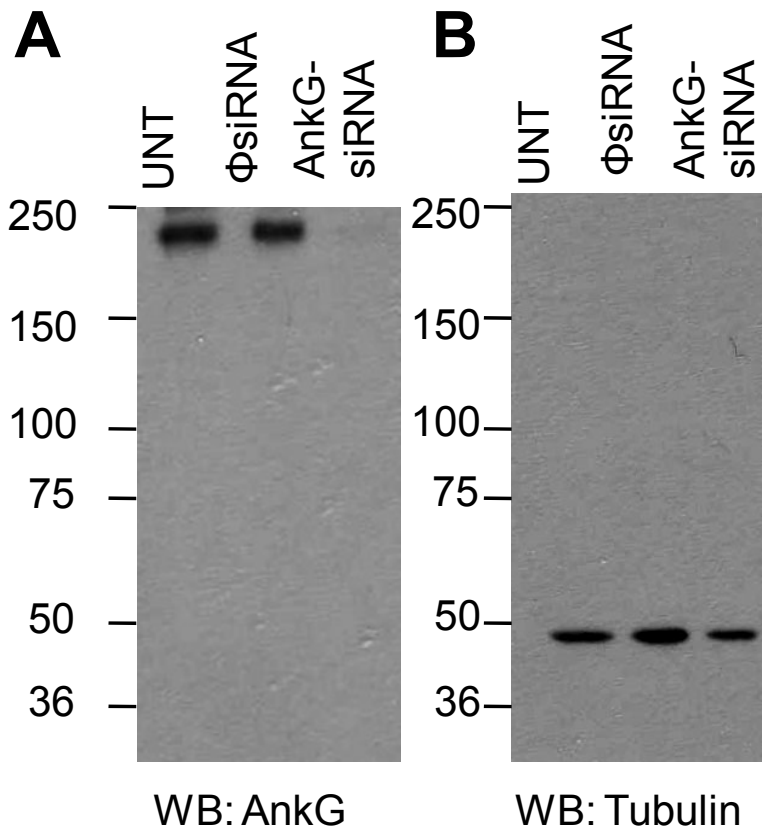

Online Figure V: Representative western blot of monolayers subjected to dispase assay under conditions of loss of AnkG expression. Samples of monolayers of NRVMs left UNT or treated with ΦsiRNA or AnkG-siRNA were probed for **(A)** AnkG and **(B)** tubulin as a loading control.

Online Figure VI

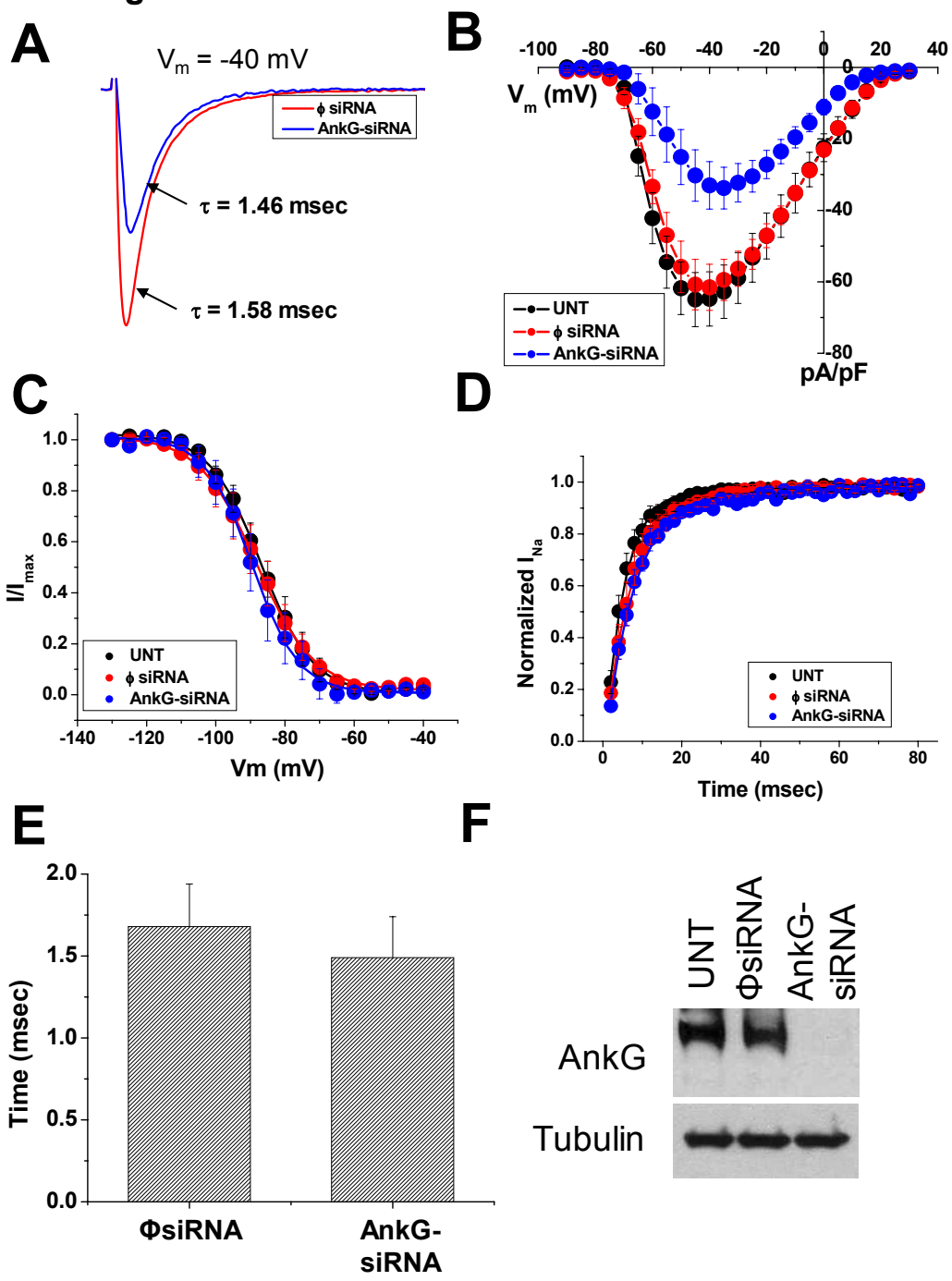

Online Figure VI: Sodium currents in NRVMs recorded ~5.5 days after introduction of AnkG silencing construct **A**: Sodium current traces obtained from NRVMs treated either with ΦsiRNA or with AnkG-siRNA, as indicated. **B:** Sodium current density after loss of AnkG. **C:** Voltage dependence of steady-state inactivation. **D:** Recovery from Inactivation. **E:** Time course of current decay. INa,peak (pA/pF) $p<0.01$ for AnkG-siRNA vs ΦsiRNA. Other comparisons were not significant. N= 7, 6 and 7 for UNT, ΦsiRNA and ANkG-siRNA respectively. **F:** Western blot for AnkG corresponding to cells used for patch clamp experiments.

Online Figure VII

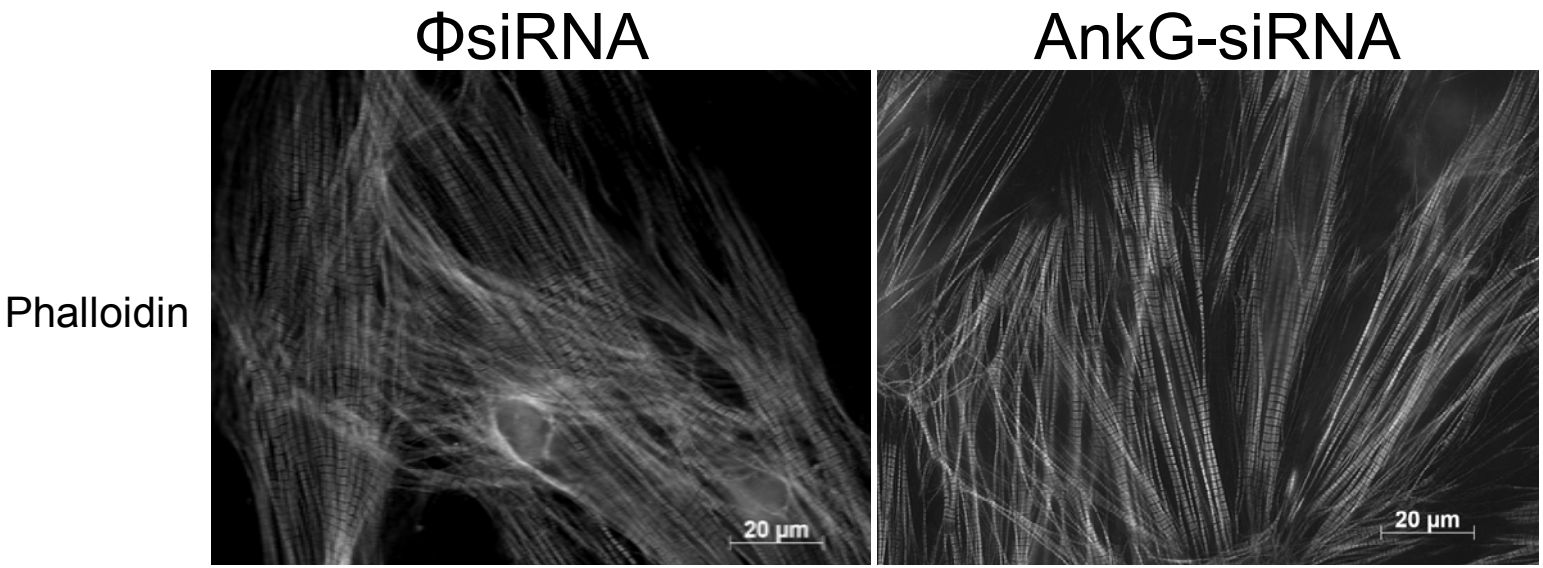

Online Figure VII: Representative immunoreactive signal for phalloidin in NRVMs treated with ΦsiRNA and AnkG-siRNA. Images acquired with 63X objective, bars=20µm.

Online Figure VIII

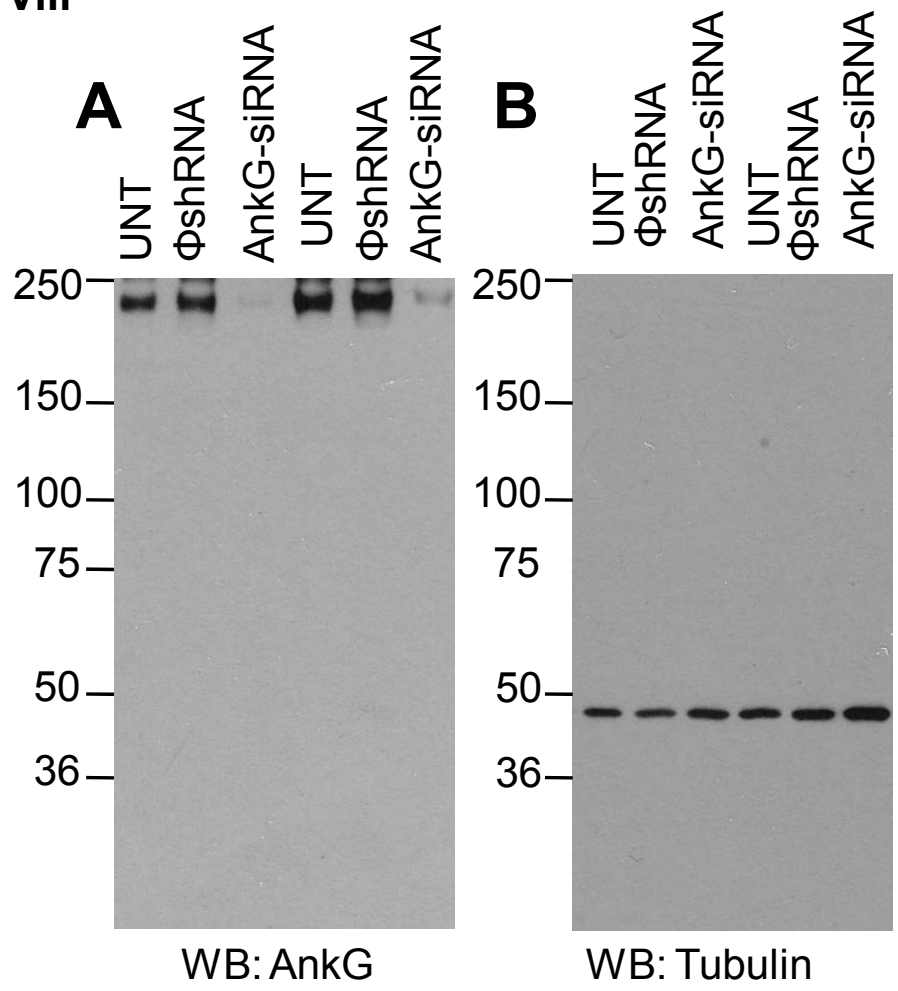

Online Figure VIII: Representative western blot of monolayers that were subjected to optical mapping. Samples of monolayers of NRVMs left UNT or treated with ΦsiRNA or AnkG-siRNA were probed for AnkG **(A)** and tubulin **(B)** as a loading control.

Online Figure IX

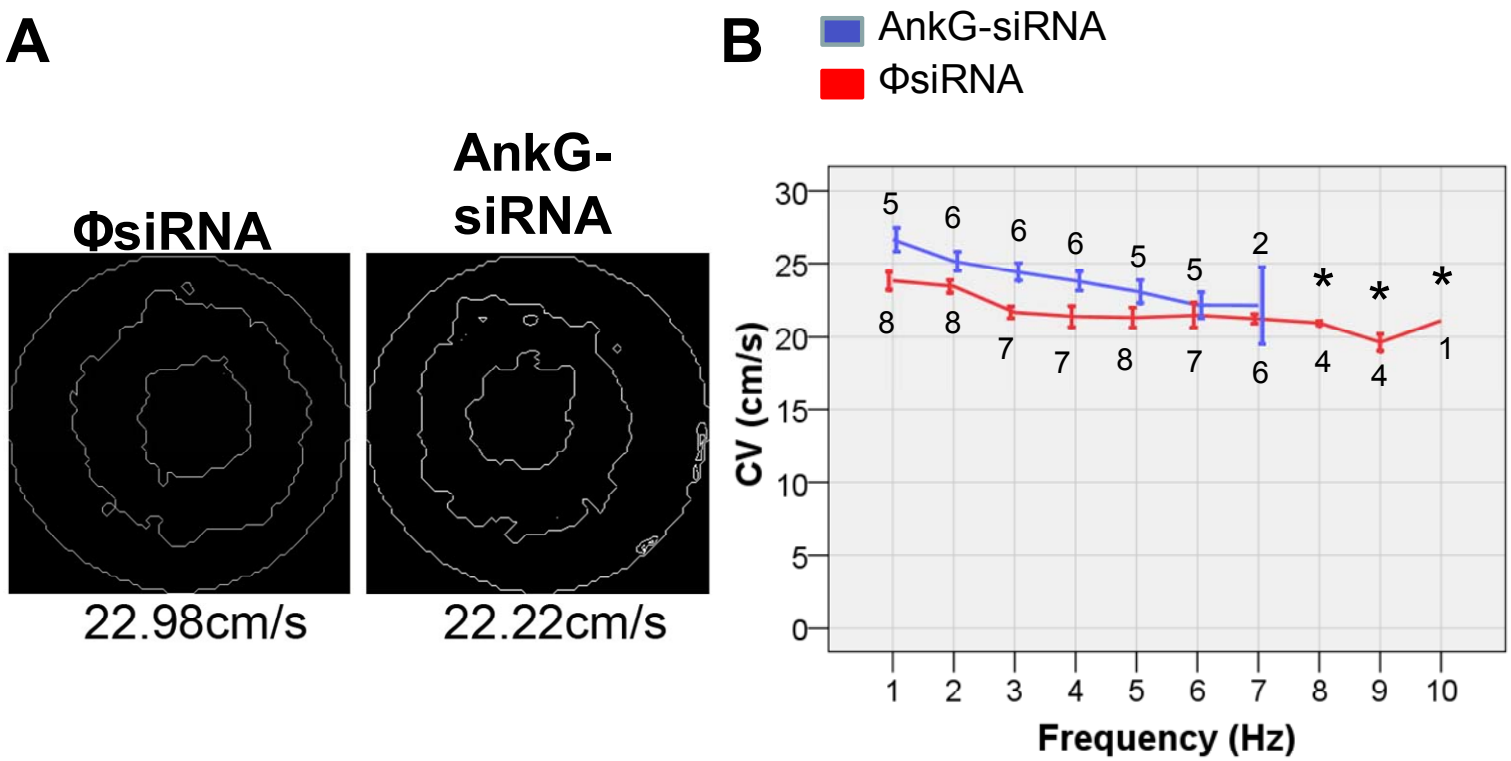

Online Figure IX: Loss of AnkG expression and action potential propagation in NRVMs. **A:** Representative isochrone maps of action potential propagation obtained by optical mapping of monolayers treated with ΦsiRNA or AnkG-siRNA. Each line corresponds to 5ms. **B:** Plot of conduction velocity as a function of pacing frequencies. Red line, monolayes treated with ΦsiRNA; blue line, AnkG-siRNA. Numbers above each point represent number of cases where 1:1 propagation was maintained during pacing at that specific frequency. Total number of preparations tested was 6 and 8 for AnkG-siRNA and ΦsiRNA groups, respectively.

Online Figure X

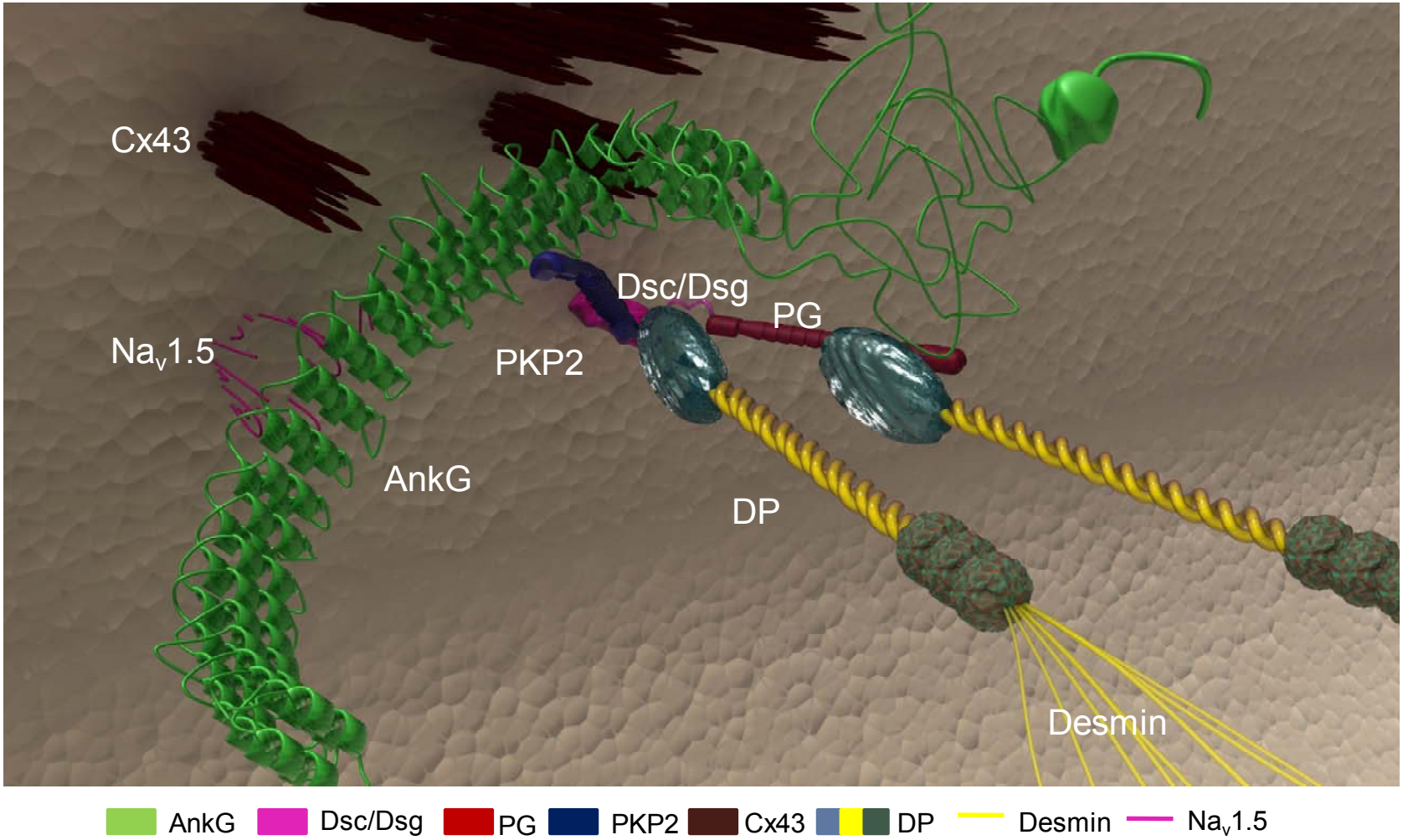

Online Figure X: Diagrammatic representation of the potential interactions between the VGSC, gap junctions, and desmosomes. Whether the interaction of AnkG with Cx43 and/or PKP2 is direct or indirect still remains to be determined